

We are IntechOpen, the world's leading publisher of Open Access books Built by scientists, for scientists

6,900

Open access books available

186,000

International authors and editors

200M

Downloads

Our authors are among the

154

Countries delivered to

TOP 1%

most cited scientists

12.2%

Contributors from top 500 universities



WEB OF SCIENCE™

Selection of our books indexed in the Book Citation Index
in Web of Science™ Core Collection (BKCI)

Interested in publishing with us?
Contact book.department@intechopen.com

Numbers displayed above are based on latest data collected.
For more information visit www.intechopen.com



Photoacoustic Imaging in Gastroenterology: Advances and Needs

*Sheena Bhushan, Sharmila Anandasabapathy
and Elena Petrova*

Abstract

Gastroenterologists routinely use optical imaging and ultrasound for the minimally invasive diagnosis and treatment of chronic inflammatory diseases and cancerous tumors in gastrointestinal tract and related organs. Recent advances in gastroenterological photoacoustics represent combination of multispectral and multiscale photoacoustic (PA), ultrasound (US), and near-infrared (NIR) fluorescent imaging. The novel PA endoscopic methods have been evaluated in preclinical models using catheter-based miniature probes either noncontact, all-optical, forward-viewing probe or contact, side-viewing probe combined with ultrasound (esophagus and colon). The deep-tissue PA tomography has been applied to preclinical research on targeted contrast agents (pancreatic cancer) using benchtop experimental setups. The clinical studies engaging human tissue *ex vivo* have been performed on endoscopic mucosal resection tissue with PA-US tomography system and intraoperative imaging of pancreatic tissue with PA and NIR fluorescence multimodality. These emerging PA methods are very promising for early cancer detection and prospective theranostics. The noninvasive transabdominal examination with PA-US handheld probe has been implemented into clinical trials for the assessment of inflammatory bowel disease. To facilitate translational and clinical research in PA imaging in gastroenterology, we discuss potential clinical impact and limitations of the proposed solutions and future needs.

Keywords: photoacoustic endoscopy, optoacoustic tomography, gastrointestinal tract, Barrett's esophagus, intraoperative, pancreatic cancer, inflammatory bowel disease

1. Introduction

Gastroenterology is a field of medicine that studies the gastrointestinal (GI) tract and its disorders. The GI tract consists of the mouth, pharynx, esophagus, stomach, small intestine (duodenum, jejunum, ileum), large intestine (also called colon which consists of the cecum, rectum, and anal canal), appendix, liver, and pancreas [1]. Imaging techniques used for the diagnosis and treatment of gastrointestinal disorders mainly include noninvasive methods (such as whole body and transabdominal imaging), minimally invasive methods (such as endoscopy), and invasive methods (such as intraoperative imaging) (**Figure 1**).

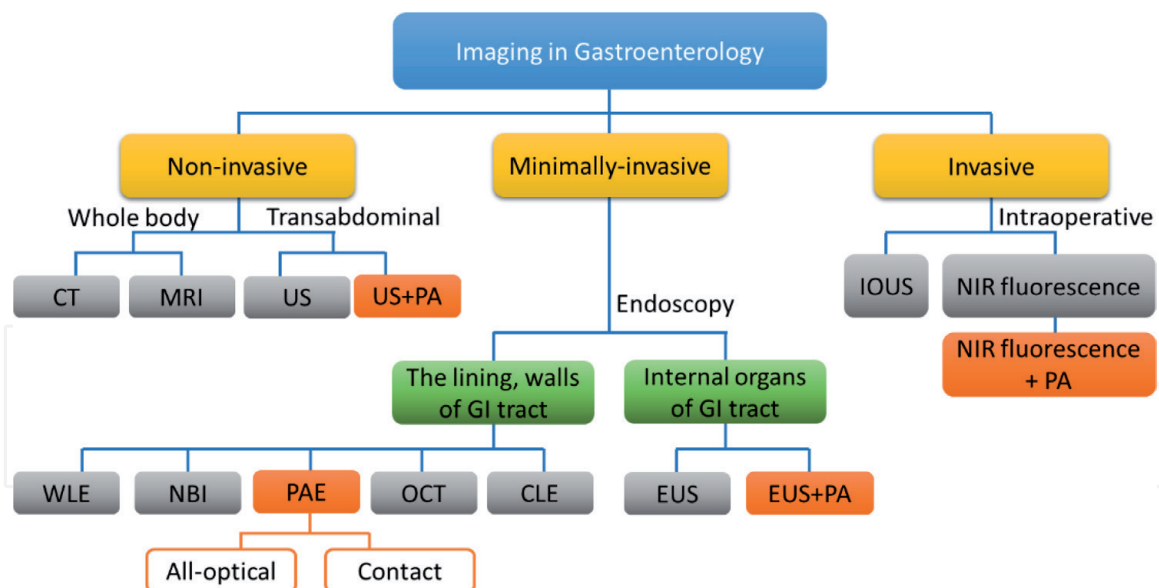


Figure 1.

Diagram of imaging modalities applied in gastroenterology: CT, computed tomography; MRI, magnetic resonance imaging; US, ultrasound imaging; PA, photoacoustic imaging; WLE, white light endoscopy; NBI, narrowband imaging; PAE, photoacoustic endoscopy; OCT, optical coherence tomography; CLE, confocal laser endomicroscopy; EUS, endoscopic ultrasound; IOUS, intraoperative ultrasound; NIR, near-infrared.

The word endoscopy is derived from the Greek words *endo* (within) and *skopein* (to see). Endoscopy is a medical procedure that employs a medical instrument called the endoscope, which is inserted directly into an organ or cavity (e.g., esophagus), thereby allowing a gastroenterologist to visualize and examine the organ's interior. Organs and cavities of the gastrointestinal tract that can be visualized and examined by endoscopy include (i) the esophagus, stomach, and duodenum (esophagogastroduodenoscopy); (ii) the small intestine (enteroscopy); (iii) the large intestine (colonoscopy, sigmoidoscopy); (iv) the bile duct and pancreas (endoscopic retrograde cholangiopancreatography, also known as ERCP); and (v) the rectum (rectoscopy) and anus (anoscopy); when both the rectum and anus are examined together, the procedure is called proctoscopy [2].

As a clinical specialty, gastroenterology relies upon endoscopy mainly for the following purposes:

- a. *To detect* pathologies like ulcers, varices, inflammation, and bleeding—which are not visible to the naked eye.
- b. *To confirm* diagnosis of cancers by taking biopsies.
- c. *To treat* pathologies in a minimally invasive manner. For example, treating a bleeding vessel by cauterization, a narrow esophagus by widening (endoscopic dilation), polyps and foreign bodies by removal, and varices by banding.

Gastrointestinal endoscopy is continually evolving to enable early detection of diseases, which can significantly impact treatment outcomes. The best-known endoscopic imaging methods in practice are (1) white light endoscopy, (2) narrowband imaging, (3) optical coherence tomography, (4) confocal laser endomicroscopy, and (5) endoscopic ultrasound. In this section, we will discuss these endoscopic imaging techniques and highlight their main advantages and limitations.

1.1 White light endoscopy

White light endoscopy (WLE) is the most commonly used endoscopic imaging modality. WLE applies the full spectrum of visible white light (400–700 nm) to visualize the outermost lining of the GI tract (also called the mucosa or epithelium) [3]. Xenon lamps are used to produce white light, which is transmitted through a filter and then reflected by the mucosa. A CCD camera then processes the reflected light to an image monitor. The image can either be of a standard resolution or can be magnified up to 150 times in the more recent versions [4]. WLE detects slight color changes on the mucosa (slight redness and pallor). However, it is incredibly challenging to detect early cancer; as in early stages, the lesion is usually unremarkable, with no significant color changes. Furthermore, WLE is limited by what the human eye can see and is often associated with low sensitivity for the detection of early neoplasia. Consequently, in attempts to increase the sensitivity of WLE, chromoendoscopy is often added. Chromoendoscopy is a technique in which special stains are topically applied to the mucosa during endoscopy. Chromoendoscopy highlights subtle irregularities in the mucosa [5], and while it can help the gastroenterologist uncover some lesions invisible to the naked eye, the specificity is often quite low.

1.2 Narrowband imaging

Narrowband imaging (NBI) is one of the most widely available optical imaging techniques today. In addition to highlighting subtle differences in the epithelium (like the combination of WLE and chromoendoscopy does), NBI can also highlight changes to the subsurface mucosal vascularization, without the use of any special stains or dyes. It can be activated by pressing a button on the endoscope, and once activated it uses special filters to narrow the wavelength range of the emitted light into blue (400–430 nm; centered at 415 nm) and green light (525–555 nm; centered at 540 nm) [6]. This system exploits the principle of depth of light penetration in accordance with the Beer-Lambert law: the shorter the wavelength, the more superficial the penetration. The blue filter is designed to coincide with the peak absorption spectrum of hemoglobin, and it enhances the mucosal vasculature, like capillaries, which appear brown under NBI. The green light penetrates deeper and enhances the appearance of submucosal vasculature, like veins, which appear cyan [7]. Computer processing can further enhance the images. Since increased vasculature is one of the earliest signs associated with cancer, NBI helps with the detection of early cancer. By helping the gastroenterologist visualize and differentiate abnormal cancer margins from normal healthy tissue, it also helps determine the mucosal areas that should be biopsied. However, NBI is not able to image submucosal abnormalities.

1.3 Confocal laser endomicroscopy

The term confocal refers to the alignment of both illumination and collection systems in the same focal plane. Confocal laser endomicroscopy (CLE) focuses blue laser light (488 nm) through a single lens on to a specific target, with subsequent detection of the fluorophores (excitable using 488 nm laser light) in the tissue through a pinhole [8]. Typically, endomicroscopes have a miniaturized scanning head at the tip of the endoscope or execute the scanning outside the patient transferring the scan pattern of the tissue through an optical fiber bundle. CLE can provide high-resolution images (~0.7–1 μm) of the GI mucosa at a cellular and subcellular level, with a field of view of ~200–300 μm [9]. By delivering real-time surrogate

“optical biopsies,” it enables physicians to interpret histology in real time. Since the first visible neoplastic changes in epithelial cancers occur at a cellular level (such as increased nucleocytoplasmic ration, irregular shape and size of the nucleus, fragmentation of nucleus, prominent nucleoli, etc.), it facilitates early detection and treatment of cancer. It allows for targeted biopsies of abnormal mucosa, thereby decreasing unnecessary biopsy as compared to WLE. Besides the esophagus and colon, it is also able to provide an optical biopsy within the pancreas [10]. Since CLE relies upon tissue fluorescence, intravenous or topically applied contrast agents (dyes) are required [11]. The major disadvantage of CLE is a small field of view (<1 mm) when compared to the area of examined surfaces (several cm).

1.4 Optical coherence tomography

Optical coherence tomography (OCT), also known as volumetric laser endomicroscopy (VLE), is a more recent endoscopic imaging technique. OCT is based on the same echolocation principle as an ultrasound but uses light waves instead of acoustic waves [12]. The OCT imager’s probe can be introduced through the accessory channel of an endoscope and be directed toward the area of interest. It is then kept in contact with the mucosal surface. OCT uses near-infrared (NIR) light (700–1500 nm range of wavelength) and directs it at the target tissue. Using an interferometer device setup, the differential light scatter is picked up, interpreted, and converted into a cross-sectional image. The typical axial resolution is around 7–10 μm which enables the cross-sectional images to provide information about the architectural morphology of the GI epithelium at a microscopic level. The lateral resolution of OCT is about 30 μm , and depending on the applied wavelength of light, depth of penetration for OCT is around 2–3 mm [13]. Since tissue is relatively transparent, the longer wavelength can penetrate deeper than CLE. However, the lateral resolution is lower than that of CLE (CLE resolution is up to 1 μm). While OCT resolution is able to detect deeper structures (e.g., crypts and glands), it cannot pick up microscopic nuclear changes, such as nuclear dysplasia. The main advantage of OCT is the deeper penetration, which would help detect cancer in the submucosal layer (the layer present right below the mucosa) [14]. On the other hand, clinical interpretation of OCT images can be challenging.

1.5 Endoscopic ultrasound

Endoscopic ultrasound (EUS) can differentiate between the various layers of the gastrointestinal tract and provide anatomical and structural details. It can employ a broad range of frequencies (5–20 MHz) to provide images with a variable depth of penetration (5–6 to 1–2 cm) and resolution (2–3 to ~0.2 mm) [15]. The most routinely used EUS array has a central frequency of 7.5 MHz. EUS is limited by a lack of specificity and an inability to differentiate between pathologies due to poor contrast (for example pancreatitis from pancreatic cancer) and is of limited use in picking up early and metastatic cancer. Additionally, EUS is a technique that largely depends on the operator’s skills and has a significantly long learning curve for novice gastroenterologists [16].

The aforementioned imaging techniques have come a long way since their inception, but are still far from perfect in several ways. Imaging that relies on WLE is substantially limited by what the human eye can see and detect on the surface, with no insight into the subsurface or cellular level. Techniques like NBI and CLE are able to provide a higher resolution but cannot reach superior depths of penetration. OCT and EUS can penetrate deeper into the tissue but are limited by poor contrast, which

makes interpretation of pathology difficult especially for early detection. Therefore, they are usually associated with low sensitivity and specificity. **Figure 2** summarizes the aforementioned optical methods of endoscopy.

The field of endoscopic imaging is continuously being upgraded in an attempt to address some of the abovementioned concerns. An emerging imaging technique known as photoacoustics (PA) may have a major advantage over other imaging modalities in both resolution and penetration depth.

1.6 Photoacoustic imaging

The basic principle of photoacoustic (aka optoacoustics) imaging is derived from the photoacoustic effect: (1) it uses a pulsed nanosecond-long laser light to illuminate a target tissue, and (2) when the energy of laser light is rapidly absorbed and followed by fast heating of material, it is converted into pressure wave via thermoelastic expansion of the targeted tissue. Using detected acoustic signals, the PA images can be reconstructed by means of algorithms of computed tomography (CT).

The amplitude of a generated PA pressure wave, p , can be described by the formula [17, 18]:

$$p = \mu_a F \Gamma = \mu_a F \frac{\beta V_l^2}{C_p}, \quad (1)$$

with the optical absorption coefficient μ_a , the local optical fluence F , and the dimensionless Grüneisen parameter Γ representing thermoelastic efficiency of the medium. The Grüneisen parameter is temperature sensitive and depends on the volumetric thermal expansion coefficient (β), the speed of sound (V_l) for longitudinal waves, and the specific heat capacity at constant pressure (C_p) [19, 20]. In the tissue, a rise of temperature $\Delta T \sim 10^{-3}^\circ\text{C}$ generates a pressure wave of $p \sim 1$ kPa.

The depth of imaging is correlated with (a) the depth of light penetration in materials and (b) the detection sensitivity of an US transducer that varies with its frequency range. Since PA imaging combines the use of light and sound, it can provide spatial resolution at the scale of optical imaging (up to submillimeter range) and a penetration depth across US dimensions (at centimeter range).

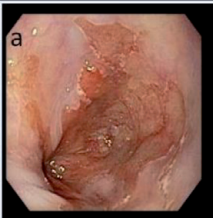
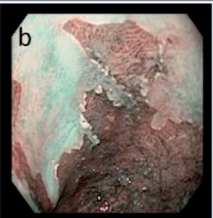
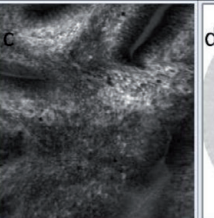
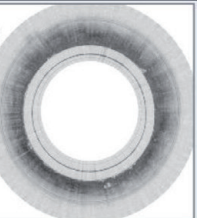
	Endoscopy		Endomicroscopy	
	WLE	NBI	CLE	OCT
Resolution	~100 μm	<100 μm	~0.7-1 μm	~7-10 μm
Depth	~10-30 μm	~300-400 μm	~300 μm	~2-3 mm
Field of view	140°	140°	~200-300 μm	~5-6 mm
Objectives	Tissue surface	Subsurface	Cellular	Architectural
Figure				

Figure 2. Comparison of endoscopic imaging modalities: (a) WLE, (b) NBI, (c) CLE, and (d) OCT (a–c) Images by Prof. Sharmila Anandasabapathy, MD. (d) Image courtesy of Prof. Guillermo J. Tearney, MD, PhD.

Resolution of PA images can be affected by multiple factors. Heat-generating optical energy must be delivered to the tissue faster than the producing pressure wave can propagate the distance equal to the desired spatial resolution. Therefore, the use of nanosecond optical pulses is a necessary (but not sufficient) condition to achieve the desirable spatial resolution. Besides, a temporal response function of a pressure-wave detector has to be not slower than the optical-pulse duration to make sure that the desirable spatial resolution is achievable.

Tissue structure can be represented by PA images only if acoustic detectors are capable to resolve rapid changes in PA signals associated with boundaries and sharp edges in tissues and reproduce slow changes associated with smooth variation in optical properties within the tissue at once. That is to say, acoustic detectors must register both high and low ultrasonic frequencies of acoustic pressure at the same time. Such acoustic detectors are called ultra-wideband acoustic transducers [18, 21].

It is challenging to detect PA signal properly. The US detection bandwidth of an acoustic transducer defines the limits of axial (depth) resolution. Furthermore, the lateral resolution of PA images is provided by an array of transducers and depends on the dimensions of each acoustic transducer and the geometry and dimensions and of the US transducers in an array. Scanning a single transducer along tissue surface can simulate the array.

In practice, PA imaging is frequently combined with conventional US detectors. At the same time, conventional US detectors have relatively narrowband characteristics due to its design to both transmit and receive acoustic wave. Spectral amplitudes of typical PA signal and US transducer parameters are illustrated on **Figure 3**.

Conventional piezoelectric transducers limit the potential axial resolution of broadband PA signals. Note that all-optical detectors of PA signal are wideband and have significant advantage in these terms [22, 23].

In general, the depth-resolution ratio defines the quality of PA imaging system. The tradeoff between depth and resolution leads to three types of PA imaging methods: microscopy (μm -scale, cellular), mesoscopy (mm-scale, microvasculature), and macroscopy (cm-scale, organs).

Scanning PA microscopy can demonstrate resolutions greater than $50\ \mu\text{m}$ (e.g., resolving capillary bed and even single erythrocytes) [24] at depths that are beyond the optical diffusion limit, something which is not achievable with conventional microscopy methods (depths are up to 4–5 mm). Additionally, spatial resolution and penetration depth are somewhat mutually exclusive in imaging techniques like the ultrasound (i.e., as the penetration depth increases, spatial resolution decreases and vice versa). PA imaging in gastroenterology mostly employs meso- and

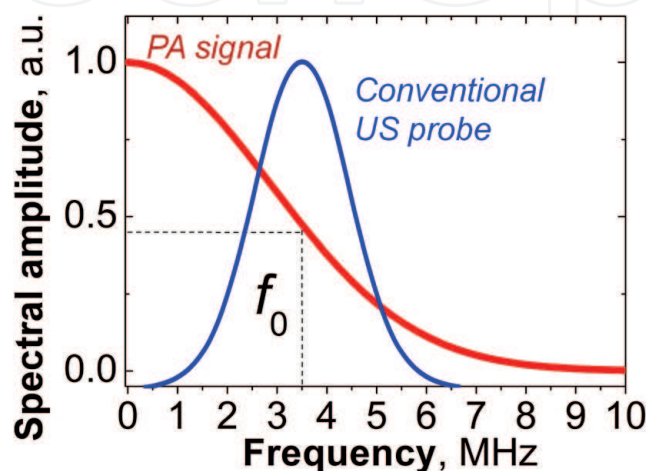


Figure 3. Spectral amplitudes of broadband PA signal and conventional US transducer.

macroscopic scale. PA deep-tissue imaging uses NIR light to generate an acoustic signal allowing for more clinically relevant penetration depth up to several centimeters, along with maintenance of spatial resolution (resolution of 0.2–2 mm at reported imaging depths of 3–7 cm) [18]. Combining clinically relevant depth with high resolution can make it possible to unmask inconspicuous “flat” lesions during early stages of cancer development. It can also help with determining the extent of the tumor depth both intraoperatively and postoperatively. **Figure 4** resumes the depth of penetration associated with the aforementioned imaging modalities on the example of the esophageal lining tissue.

Unlike other imaging modalities, PAI can use endogenous chromophores such as oxyhemoglobin, deoxyhemoglobin, lipid, water, and melanin. The NIR light has longer wavelengths (700–1000 nm) than the visible light range, and these wavelengths can be used to reach deep within the tissue and provide detailed information about its composition. In addition to revealing normal physiological characteristics (total hemoglobin concentration, O₂ saturation of hemoglobin, blood flow, temperature), it can help physicians detect hypoxia, perfusion, and increased vasculature (also called neoangiogenesis—which is an early sign of cancer) through *anatomical* and *functional* imaging, relying exclusively on endogenous contrast agent (without dyes). Exogenous agents can also be used to provide *molecular* imaging, to enhance the contrast further, and to facilitate deeper penetration. They can be used in a targeted manner to target molecular-specific processes, such as biomarkers specific to inflammation or certain type of tumors. For example, cancer development is associated with increased permeability of the vasculature, which leads to extravasation of the contrast agent use. Overall, by providing a high optical contrast, it helps differentiate the cancer margin from the surrounding healthy tissue in real time. Lastly, it is quite similar and also naturally compatible with the ultrasound in

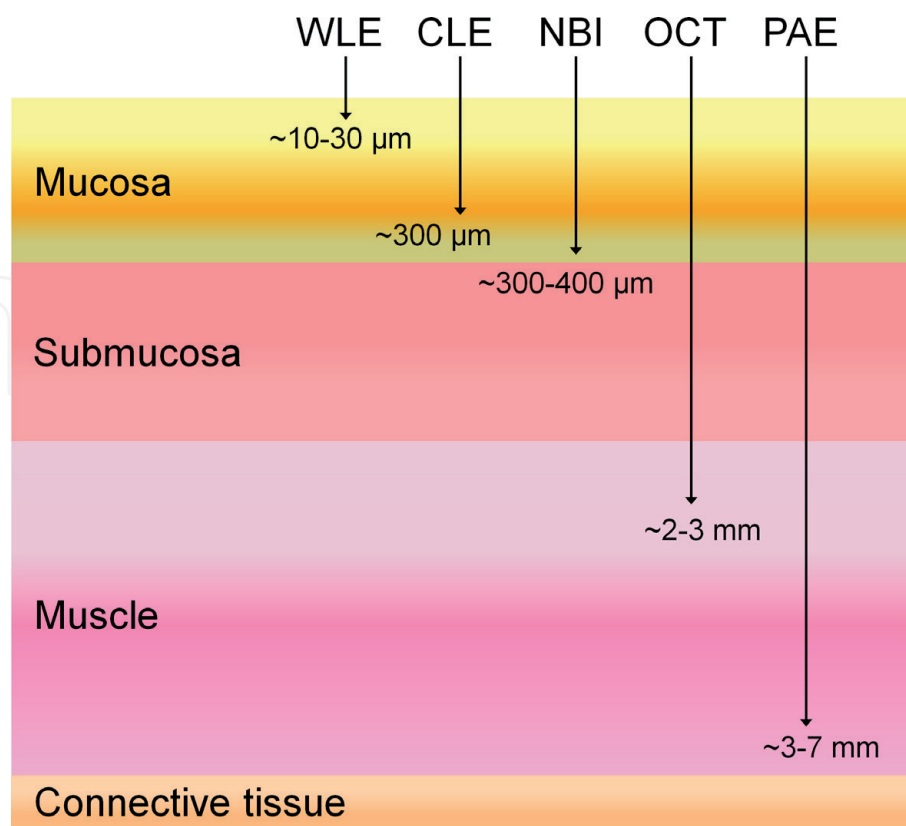


Figure 4. Schematic summarizing the depths of penetration into esophagus tissue for routine and emerging imaging techniques.

principle and operation. It is portable and can be used in real time and requires no special training. It does not utilize ionizing radiations and is therefore minimally invasive and safe, making it an easily adoptable technology for physicians. In the upcoming sections of this chapter, we will discuss most recent PA imaging applications for gastroenterology.

2. Applications of photoacoustic imaging in endoscopy

2.1 Esophageal cancer

Esophageal adenocarcinoma carries a significant disease burden in the Western world. Barrett's esophagus (BE) is the most important risk factor for developing esophageal adenocarcinoma. Patients with BE are at 30- to 125-fold increased risk of developing cancer than the general population [25]. Patients who develop high-grade dysplasia (HGD) from BE have an even higher chance of developing esophageal adenocarcinoma [26]. Indeed, early detection of Barrett's esophagus significantly improves treatment outcomes, yet accurate detection of dysplasia in BE still remains a challenge. In BE, the normal esophageal squamous mucosa (which appears white under WLE) is replaced by an intestinal-type columnar mucosa (appears salmon pink under WLE). The current standard of care includes taking targeted biopsies of visible lesions under WLE guidance, which are then sent over to histopathology for staging. However, since this approach cannot sample the entire esophagus, the chances of missing dysplasia (precursor to cancer) are very high [27]. Additionally, the screening is just limited to the mucosa, making detection of submucosal invasion impossible.

Indeed, techniques like NBI and CLE yield high-contrast, subcellular images, but they fall short in terms of depth (1.5–2 mm) [28], which is not sufficient to detect submucosal invasion. Tumors that have invaded the submucosa are treated by surgical removal of the esophagus (esophagectomy) which is often associated with significant mortality and decreased quality of life, whereas tumors that have not yet invaded the submucosa can be treated by less aggressive techniques like endoscopic mucosal resection (EMR). There is a clinical need for developing an imaging modality that can detect dysplasia *in vivo* and also image beyond the mucosa layer into the submucosa. Since PA microscopy can provide high-resolution imaging of the microvasculature, it can help to bridge these gaps by helping physicians to differentiate between nondysplastic and dysplastic BE early on. Additionally, it is also capable of imaging deeper into the tissue (up to 3–5 mm) and reaching the submucosal layer, thereby also helping with staging of the cancer in real time. In the next section of this chapter, we will talk about an *in vivo* preclinical and an *ex vivo* clinical study that used PAI to help detect esophageal cancer.

2.1.1 Noncontact, all-optical photoacoustic endoscopy

A miniature, all-optical, forward-viewing PA catheter for high-resolution 3D endoscopy was developed by Ansari et al. [29]. The sensor provided the necessary broadband (1–70 MHz), well-behaved frequency response for faithfully recording the wideband acoustic frequency spectrum of photoacoustic waves. A 3D image had a cylindrical field of view of 3.5×7 mm; the diameter of the catheter was 3.2 mm. The lateral resolution ranged from 40 μm at a depth of 1 mm to 175 μm at a depth of 7 mm. These variations arise because the solid angle that is subtended by the absorbers to the FP sensor plane decreases as the depth increases. The first tests were performed on highly vascularized tissue samples and demonstrated great

potential of the method (**Figure 5**). Excitation laser wavelength, 590 nm; pulse repetition frequency, 30 Hz; and incident fluence, 15 mJ/cm^2 , which is lower than the American National Standards Institute (ANSI) laser safety limit (20 mJ/cm^2), were used.

The microvasculature can be seen very well. The data acquisition time was as long as 25 min and cannot be considered as clinically relevant; though, in the future this parameter can be improved applying a faster laser with pulse repetition rate up to 200 Hz and parallelizing readout of the sensor. The technique described above addressed some of the needs for early diagnostics of esophageal cancer (since BE is associated with increased vasculature) and demonstrate capability to image partially submucosa. However, to the best of our knowledge, no examination of this method was performed on esophagus so far either in vivo or ex vivo.

2.1.2 Catheter-based photoacoustic ultrasound endoscopy

The use of contact (coupling required) multimodal photoacoustic and ultrasonic endoscopic imaging to two rabbit esophagi, to investigate the esophageal lumen structure and microvasculature, was demonstrated by Yang et al. [30]. Both in vivo and ex vivo studies were performed, and high-resolution photoacoustic images of vasculature network in the walls of GI tract were acquired and analyzed. To perform this experiment, they used a catheter-like side-viewing photoacoustic endoscope/endoscope ultrasound miniprobe (PAE-EU). This setup allowed to image internal walls of the GI tract using both PA and US simultaneously. A wavelength of 584 nm with a laser energy of 0.3 mJ/pulse was used to produce PA image contrast proportional to the hemoglobin concentration. The detection transducer was fabricated as $\sim 36 \text{ MHz}$, 65% fractional bandwidth that allowed a penetration depth of up to 3.5 mm. The field of view of the endoscopic scanning system was 7 mm, and its angular field of view was set to 270 degrees. A focused US transducer detected 1D depth-resolved signals (or A-lines), and cross-sectional images (or B-scans) were produced using rotation of a scanning mirror that directed optical and acoustic waves. Data acquisition system collected dual-wavelength photoacoustic and

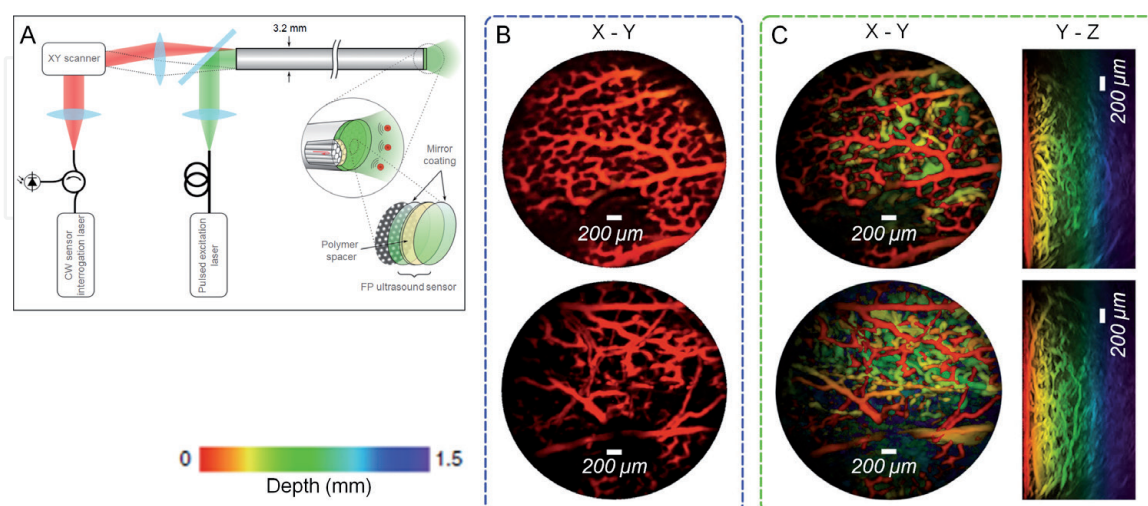


Figure 5. (A) Schematic of the all-optical forward-viewing PA endoscopy probe includes the magnified distal end of individual fiber-optic cores in the coherent fiber bundle and ultrasound sensor based on the principle of Fabry-perot (FP) interferometer. (B) High-resolution PA images of ex vivo capillary network of the chorioallantoic membrane that surrounds the avian embryo. X-Y maximum intensity projections (MIPs) for depth range $z = 0\text{--}200 \mu\text{m}$ of two regions on the same sample with the microvascular anatomy. (C) X-Y MIPs for the depth range $z = 0\text{--}1.5 \text{ mm}$ for the same two regions as Panel B, respectively, and Y-Z MIPs. The images are reproduced from open-source publication [29] with author permission.

the inferior vena cava, aorta, and parts of the pulmonary vasculature were visible. Unfortunately, following the correction, the finer vessels were blurred out and were not visible.

Ex vivo imaging results: the absence of motion artifact in the ex vivo experiments enabled the acquisition of higher-quality, uninterrupted 3-D maps of the esophageal vasculature. The PA data was clearer, stronger, more detailed, and overall superior than the US data. Vascular structures (both major and feeding vessels) were clearly visible, whereas in US the smaller vessels were not as clear. Using PA, the group was also able to measure the blood vessel diameter, based on the PA esophagus distance maps. On comparing PA and US images with histology, it was found that the PA images provided clear boundaries of the esophageal wall, consistently throughout the length of the esophagus. This can be attributed to a strong PA signal generated by the capillary dense submucosal layer. However, the US did not show clear boundaries of the mucosal and submucosal layers consistently, mainly due to weak signal intensities in these layers. Wall thickness of the esophagus calculated using PA varied only slightly from the histological images (PA were thinner than histological images). This slight change can be attributed to distortion of the tissue during histological fixation. Thorough analysis of PA-US overlapped images made it possible to identify the submucosal layer of the esophagus along with the surrounding vasculature like the aorta and inferior vena cava [30]. Thus, PAE can provide label-free visualization of microvasculature (as small as 190 μm), which exceeds the capability of current EUS technique in the esophagus. While Doppler ultrasonography can image blood vessels, it can only image large blood vessels which lowers its sensitivity. Since PAE can image smaller blood vessels, it is far more sensitive and could prove to be an invaluable asset for diagnosing BE. Moreover, PAE can also visualize vasculature in the surrounding mediastinal region, which can prove helpful intraoperatively (during esophagectomy). Since a majority of modern endoscopes have narrow working channels, further miniaturization of the tool to about 2.8 mm in diameter is required. Furthermore, if motion artifacts can be decreased, this technique can be used not only for diagnosing BE but also for guiding surgical procedures like esophagectomy. Motion artifacts can be reduced by increasing the scanning speed and by adding respiratory gating to the image acquisition. Next, we will talk about an ex vivo study that was done in human samples.

2.1.3 Ex vivo endoscopic resection tissue with PA tomography system

An ex vivo feasibility study in humans that used PA imaging in patients undergoing EMR for dysplasia was conducted by Lim et al. [31]. The aim of this study was to identify microvascular patterns associated with dysplasia in ex vivo samples, with the long-term goal of performing in vivo PA imaging for the detection of dysplasia in patients. In this study, a commercially available photoacoustic tomography imaging system Vevo LAZR (VisualSonics, Toronto, Ontario, Canada) was applied. A linear-array US transducer of 40 MHz central acoustic frequency and 256 elements (LZ550, VisualSonics) were integrated with fiber-optical bundles to provide a cross-laser-beam geometry for optical excitation. Photoacoustic and US images were recorded and displayed at a frame rate of 5 Hz. PA and US scans were obtained from a total of 13 ex vivo EMR samples from 8 patients. Excised tissues were mounted using ultrasound gel onto a plastic dish filled with gelatin (5% weight of 40 mL volume) to minimize acoustic signals from the dish. Because of the cross-laser-beam geometry of the PA imager fiber bundle attached to the transducer, there was an optimal photoacoustic zone located between 9 and 11 mm in front of the probe. Hence, they positioned the top surface of the tissue at 9 mm for consistency between samples.

PA imaging scans were made at each wavelength of 680, 750, and 850 nm. Additional measurements were made at 824 and 970 nm in anticipation of future work, in which this data would serve as controls in studies of topical biomarker-targeted porphyrin-lipid nanoparticle contrast. The transducer was mounted onto a motorized translational stage and scanned over a 3D volume at ~ 0.06 mm step size. The PA imaging laser power was below the ANSI maximum permissible exposure for skin (20–70 mJ/cm² for 680–970 nm), avoiding any tissue heating that might damage the tissue, as confirmed on subsequent histopathology. Once data acquisition was completed, the specimen was marked and sent for histopathology.

The relative concentrations of oxyhemoglobin (HbO₂) and deoxyhemoglobin (Hb) were estimated by PA imaging intensity using two wavelengths of 750 nm and 850 nm. The relative total hemoglobin was then given by the sum of relative HbO₂ and Hb values. PA images were used for a 3D reconstruct of the complete EMR tissue. The US provided structural information, while the PA imaging provided functional information about the distribution of endogenous absorbers (blood) within the tissue. While there were no differences seen relative hemoglobin (HbT) among the various subclasses of BE, a higher relative HbT was seen in BE as compared to normal squamous mucosa. Since BE is associated with increased vasculature, it makes sense that it appears salmon pink under WLE (whereas normal tissue appears white). Even though this study did not utilize submucosal tissue, PA imaging data was detected beyond 2 mm from the tissue surface. A major limitation of this study was that distinction between dysplastic BE and nondysplastic BE could not be made on resected tissue. Further studies are needed to find out if PA imaging can help detect dysplasia. However, owing to its penetration depth capability, PA imaging can be very useful for endoscopic cancer staging. Note that the selection of more optimal PA imaging system also can improve the outcome.

2.2 Inflammatory bowel diseases

Inflammatory bowel disease (IBD) is widely prevalent and carries a significant burden around the world [32]. While the diagnosis is usually a clinical one, colonoscopy is performed for confirmation. Patients with a long-standing history of the disease (8–10 years) are at a higher risk of developing colorectal cancer. Annual screening colonoscopies are advised to detect early cancer changes (dysplasia) and to monitor the status of the disease in these patients. Colonoscopy is a minimally invasive but uncomfortable procedure that is necessary in this patient population. Real-time multispectral optoacoustic tomography (MSOT) imagers can detect the oxygenated and deoxygenated hemoglobin in tissue, thereby allowing physicians to detect structural and vascular changes associated with IBD in a noninvasive manner. More recently, MSOT can use combined photoacoustic and ultrasound signals, which further improves its radiologic capabilities. In this section we will discuss three studies that used MSOT to study IBD. First, we will talk about a preclinical study that used MSOT to study inflammatory and early cancer changes associated with IBD, in mice.

2.2.1 Preclinical studies

Bhutiani et al. [33] tested the usefulness of this MSOT to assess inflammatory and dysplastic changes associated with IBD, in bowel murine models. The goal of the study was to assess diagnostic capability of PA imaging of endogenous contrast agent (hemoglobin) for inflammation of the GI tract organs in preclinical model. A total of 9 mice were imaged from the thorax to the pelvis using the preclinical MSOT system inVision 256 TF (iThera Medical). Wavelengths of 680, 710, 730,

740, 760, 770, 780, 800, 850, and 900 with an acquisition time of 10 ms per frame were used for imaging. Imaging was done at three time points, the first one was before bacterial inoculation, the second one was done 2 days post bacterial inoculation, and the final imaging was done 7 days post bacterial inoculation. The images were reconstructed through back projection with 75 μm resolution. Following imaging, colonoscopy was performed on the mice, and a Colitis Severity score was obtained using a standard severity index. After colonoscopy, the mice were euthanized, and samples from their colons were taken and sent for histopathology.

The mice in the experimental group, who had bacterial-induced colitis, showed an increased mesenteric and colonic vascularity. An increase in the mean signal intensity of oxygenated hemoglobin by MSOT was also observed in the experimental group as compared to the control group. The intensity of the signal was mild at time point two (i.e., 2 days post bacterial inoculation) and was most remarkable at point three (i.e., 7 days post bacterial inoculation). The deoxygenated signal obtained through MSOT showed no difference between the two groups at any time point. The findings on MSOT were confirmed by the colonoscopy findings. The mice in the experimental group, who had bacterial-induced colitis, had higher colitis score than the control group at time point two (2.5 vs. 1.5). At time point three, i.e., 7 days post bacterial inoculation, the experimental group had an average score of 5.5 with visible vascular and structural changes. Both the MSOT and colonoscopy findings were also confirmed by histopathology. Mice in the experimental group showed increased infiltration by inflammatory cells along with architectural destruction, at both time points two and three. We will now discuss two clinical models that used MSOT to assess changes associated with Crohn's disease in humans.

2.2.2 Clinical studies

Using clinical, handheld probe MSOT, intestinal inflammation in 91 patients with Crohn's disease (ClinicalTrials.gov number, NCT02622139) was detected transabdominally as reported by Knieling et al. [34]. MSOT was used to assess hemoglobin levels in the intestinal walls of patients with active and non-active Crohn's disease. Using clinical, endoscopic, and histological scorings, patients were classified into two groups: patients who had active Crohn's disease (inflammation) and patients with no active disease (no inflammation). Ultrasonography was also done, following which the patients underwent MSOT imaging. Comparisons were made between the distributions of MSOT measurements between the two groups (patients with active Crohn's vs. non-active disease). The diagnostic performance of MSOT was also compared with that of ultrasonography. It was found that there was a significant difference in single wavelength measurements at 760 nm and spectrally unmixed total hemoglobin between patients in remission and those with active disease. While this study was limited by a small sample size, it suggests that MSOT can be used to differentiate patients in remission from those with the active disease. If patients are in remission, they do not need more invasive procedures (**Figure 7**).

In another set of experiments conducted by Waldner et al. [35], as a part of the same clinical trial (ClinicalTrials.gov number, NCT02622139), MSOT was used as rapid, noninvasive method to assess disease activity in patients with Crohn's disease. CD activity was determined based on clinical, endoscopic, and histologic evaluation along with ultrasonography. A handheld MSOT device (3–4 MHz, 256 transducer) was placed on the abdominal wall and used to provide images of the intraabdominal organs. B-mode ultrasound imaging was used in conjunction to localize parts of the intestine for accurate photoacoustic measurements.

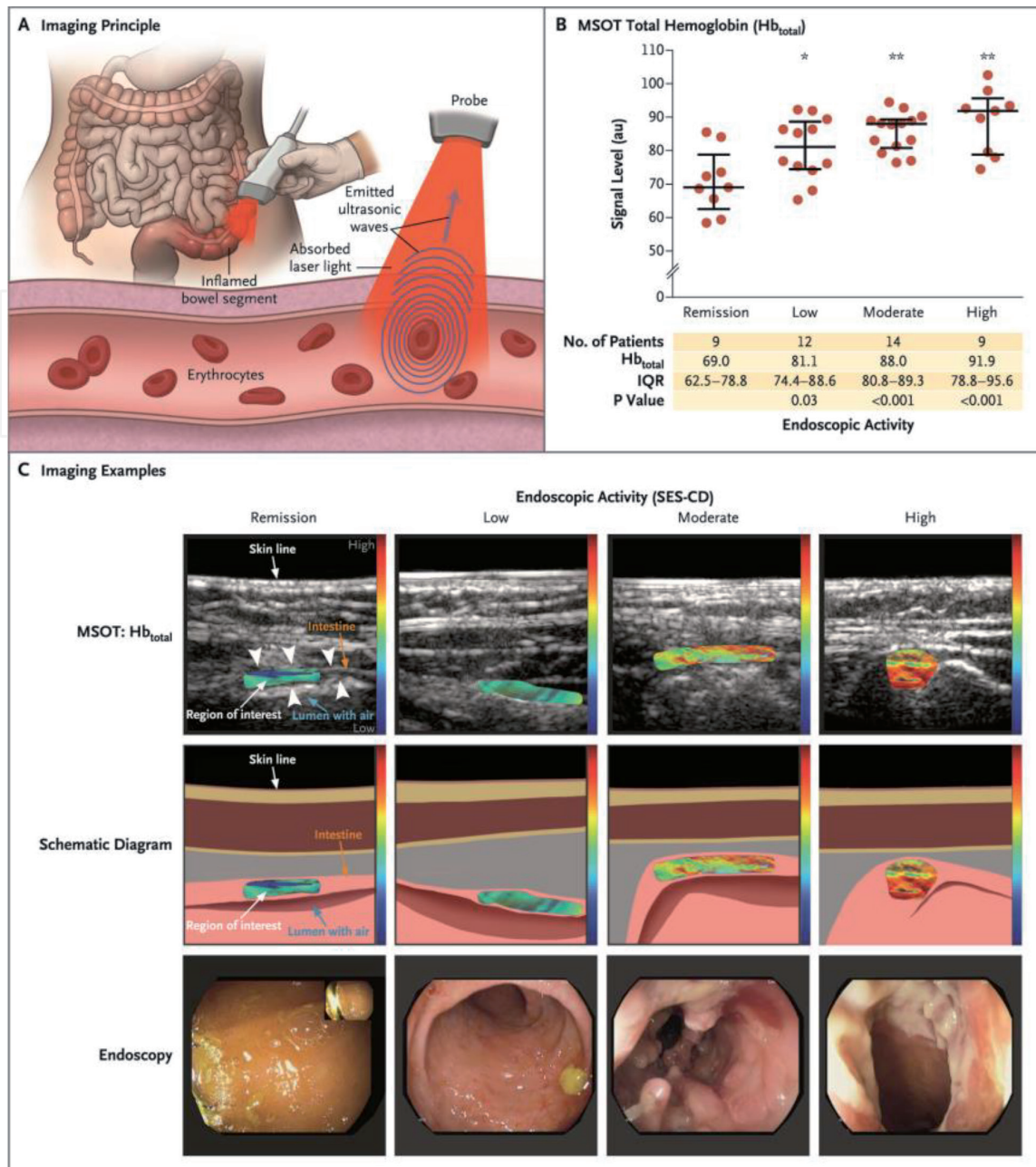


Figure 7. Multispectral photoacoustic tomography for the assessment of Crohn's disease activity. (A) Transabdominal imaging method using handheld US probe upgraded with laser light illuminators. PA data were acquired at the wavelengths of 700, 730, 760, 800, 850, and 900 nm. MSOT system calculated total hemoglobin (Hb_{total}), oxygenated hemoglobin, deoxygenated hemoglobin, and oxygen saturation to evaluate tissue perfusion and oxygenation as factors of inflammation. (B) Normalized signal level indicated Hb_{total} in the intestinal wall of both the large bowel and the small intestine as a function of endoscopic inflammation degree. Simplified endoscopic score for Crohn's disease (0–56) was applied to evaluate severity of intestinal inflammation: Remission <3; low disease activity 3–6; moderate disease activity 7–15; high disease activity >16. IQR is the interquartile range; a single asterisk points to $P < 0.05$ and a double one to $P < 0.001$. (C) The top row represents pseudocolored maps of Hb_{total} in the large bowel and small intestine with an overlay of US images. The middle row exhibits schematics of the top row images. The bottom row demonstrates the corresponding endoscopic images used for evaluation of inflammation. The images are reproduced from [34]. Copyright © 2017 Massachusetts medical society. All rights reserved.

MSOT signals were acquired with 700-, 730-, 760-, 800-, 850-, and 900-nm excitation wavelengths. Results showed that Hb_{total} , HbO_2 , and SO_2 continuously increased and correlated well with disease activity. Since MSOT signals can be obtained within 5 minutes, this technique can be used as a rapid, noninvasive way to assess disease activity in patients with Crohn's disease.

MSOT offers many advantages over the current imaging modalities. It is portable and noninvasive with a high depth of tissue penetration (up to 5 cm). It does not

require contrast agents and quantifies oxygenated hemoglobin, to inform physicians about inflammatory and vascular changes associated with IBD. Therefore, it can be used as a noninvasive objective assessment tool not only to diagnose IBD but to also monitor its severity, progression, and transformation into cancer. Small changes in MSOT imaging can prompt physicians to alter treatment course and possibly also help with early detection of cancer. Finally, since it is noninvasive and less uncomfortable than a colonoscopy, it is also likely to be accepted by patients.

2.3 Pancreatic cancer

Pancreatic cancer is the seventh leading cause of cancer-related mortality worldwide [36]. The 5-year survival rates are <7%, mostly due to a delayed diagnosis and ineffective treatment methods [37]. Treatment is usually done by surgical resection of the tumor, and only 20% of patients are eligible for resection at their initial diagnosis, due to locoregional spread and metastasis [38]. The 5-year survival rates can be significantly improved if the diagnosis is made at an early stage (no metastasis) and if the patient has cancer-free margins post-surgery [39, 40]. When the diagnosis is made at an early stage, the tumor is usually small, well defined, and localized. During surgical resection of the tumor, the surgeon aims to remove the entire cancerous tissue (to get cancer-free margins); however, margin-positive resections occur very frequently (up to 70% of PDAC cases) [41]. Due to the growth pattern of the tumor and inability to differentiate between normal and cancerous tissue, small tumor extensions are usually missed during surgery. This increases the chances of metastasis post-surgery which impacts long-term survival rates negatively.

The current imaging modalities used for diagnosis and treatment are X-ray radiography, transabdominal ultrasound, endoscopic ultrasound, computed tomography, magnetic resonance imaging (MRI), positron emission tomography (PET), and single-photon emission computed tomography (SPECT). While sensitivity for detecting tumors larger than 2 cm is very high with modalities like CT, the sensitivity for tumors less than 2 cm is only 77% [42]. Imaging techniques like ultrasound, CT, and MRI detect structural and anatomical changes in the pancreas. They cannot detect molecular changes, and since it takes years of molecular changes for the structural changes to manifest, these imaging techniques have low specificity for early detection of pancreatic cancer. Molecular imaging techniques like PET and SPECT offer more sensitivity and specificity. But PET and SPECT involve ionizing radiation and thus are harmful to living organisms. Another major limitation of the conventional imaging techniques is that most of them cannot be employed as intraoperative imaging tools [43].

The only tools currently available intraoperatively to assist the surgeon with resection are intraoperative ultrasound (IOUS) and intraoperative frozen section analysis (IFSA) by a pathologist. IOUS helps the surgeon to anatomically differentiate cancerous tissue from the surrounding structures [44, 45]. It provides high-resolution, real-time intraoperative imaging and helps determine resectability of the tumor [44]. However, it is not as reliable for detecting smaller superficial lesions [46]. Additionally, it requires considerable amount of training and experience both for operation and for interpretation [47]. IFSA also helps determine resectability of the tumor, when locoregional spread is identified. It helps the surgeon to ensure negative margins after resection [48]. However, it is time-consuming and associated with high false-negative results [49, 50]. The inability to accurately identify tumors intraoperatively can lead to incomplete resections, which results in metastasis post-surgery. Additionally, patients with undetectable micrometastasis, who are not eligible for resection, may undergo unnecessary surgeries without any impact on the outcome. Thus, there is a need for

newer imaging techniques that can help with early detection of pancreatic cancer and also help stratify patients better for treatment. Since PA imaging combines the use of light and sound waves, it can provide real-time, high-resolution, functional, and molecular imaging without ionizing radiation—a significant advantage over the other imaging techniques like CT, PET, and US. As previously discussed, PA imaging also allows penetration up to clinically relevant depths, thereby making it a favorable imaging tool that can be used intraoperatively. Additionally, when used in conjunction with tumor-targeting molecular agents, it has the potential to provide crucial information to the surgeon during intraoperative use. Lastly, PA imaging is very complementary both to US imaging and fluorescence imaging and can be easily adopted by gastroenterologists.

2.3.1 Preclinical studies on diagnostics

Using exogenous agents in PA imaging can further enhance its diagnostic capabilities. Homan et al. [51] developed a PA contrast agent—silver-silica nanocages (180–520 nm in diameter), to enhance PA imaging in pancreatic tissue. The nanocages were injected into the ex vivo porcine pancreas which were then imaged using a combined PA and US benchtop experimental setup (PA-US). The PA-US used an 800 nm light with a 7 ns pulse duration at a 10 Hz repetition rate. Optical fibers were symmetrically bundled on two sides of the US linear transducer array with 7 MHz center frequency, 14 mm wide, and 128 channels, and this arrangement allowed to produce PA and US images along the same plane. The imaging results showed that nanocage contrast agents enhanced PA imaging contrast.

Further, Homan et al. [52] also used silver nanoplates as PA imaging contrast agent to conduct in vivo PA and US imaging in transgenic mice with orthotopically grown pancreatic cancer. At first, PA and US images of the tumor were obtained without the nanoplates. Subsequently, silver nanoplates were injected into the tail vein, and imaging was done every hour following the injection, up to a total of 6 h. PA signals were captured in the wavelengths of 740–940 nm to differentiate the signals from blood and nanoplates using known optical spectra. A 3-D reconstruction of the orthotopic tumor was made, and a heterogeneous distribution of nanoparticle accumulation in the tumor was noted. These findings were confirmed on histology. Because silver nanoparticles accumulate in the tumor and can provide contrast-rich images of the tumor using PA imaging, they have tremendous potential particularly in studying the molecular profile of pancreatic cancer.

Dai et al. [53] conducted a study in which they used in vivo murine models to obtain molecular images of pancreatic tumor at transmission (forward projection) mode of PA imaging. They used multimodal endoscopic approach combined with targeted multifunctional iron oxide nanoparticles (IONPs). The authors evaluated the efficiency of the proposed biomarkers to identify margins of pancreatic tumor using contrasted PA imaging and compared to NIR fluorescence. Results showed that the contrast between the tumor and normal tissue was very low to identify the tumor with nontargeted molecules (NIR830-IONP), whereas tissue with targeted molecules (NIR830-ATF-PEG-IONP) showed greater contrast between normal and cancerous tissue. Additionally, the tumor margins were clearly demarcated. The use of targeted multifunctional nanoparticles significantly improved the signals of the tumor.

2.3.2 Clinical studies on intraoperative photoacoustic imaging

An intraoperative use of PA imaging that targets the epidermal growth factor receptor (EGFR) was described by Tummers et al. [54]. EGFR a transmembrane

receptor is highly expressed in pancreatic cancer and hence can be used as a target for fluorescence imaging. Patients with pancreatic cancer, who were eligible for resection, were given a pretreatment dose of unlabeled cetuximab, which saturated the EGFR receptors in normal tissue with high expression. This also helped differentiate between a cetuximab reaction and a cetuximab-IRDye800 reaction. Thereafter, patients underwent surgery. During surgery, the abdomen was first imaged using laparoscopic optical imaging system (NIR imaging), which was followed by resection of tumor. Following resection, all excised tissues underwent ex vivo photoacoustic imaging. Lastly, the samples were sent for histopathological correlation. Results showed that during laparoscopic NIR imaging, the pancreatic tumor and lymph nodes would be identified in all patients (6/6). Using fluorescence imaging, a clear contrast was seen between the tumor and surrounding tissue for pancreatic cancer and lymph node dissection. Ex vivo photoacoustic images showed an increased PA signal in the primary tumor tissue as compared with the surrounding pancreatic tissue and in tumor-bearing LN. A difference in signal-to-noise ratio was also observed. Both these findings were consistent with the fluorescence imaging results in the same patients.

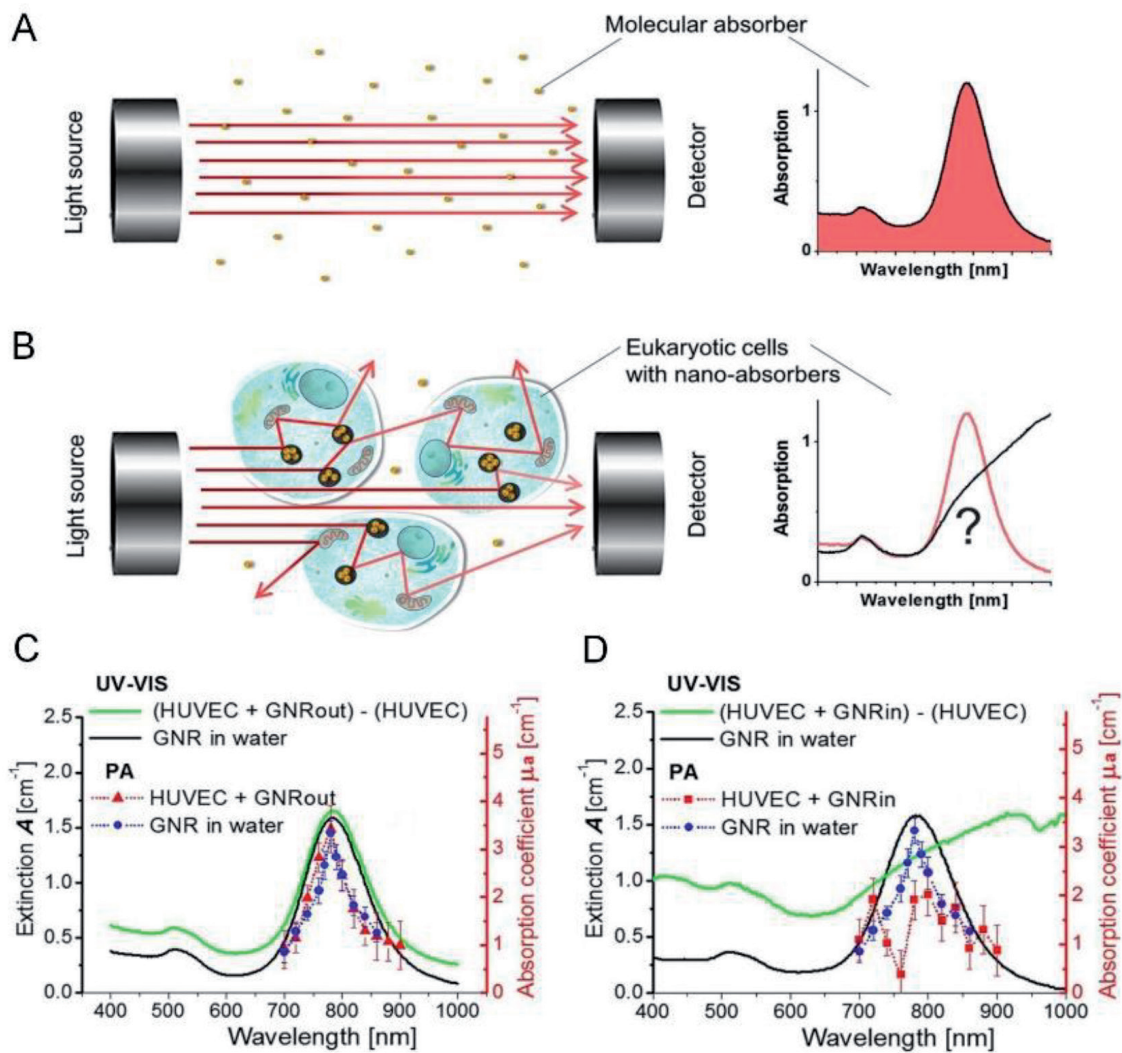


Figure 8. (A) Absorption spectrum detected with UV-VIS spectrophotometer when light is attenuated only via molecular absorption. (B) UV-VIS spectrum when light is attenuated (i) due to molecular absorption by contrast nanoagents after its cellular uptake and (ii) a part of the incident photon flux is scattered. (C and D) absorption spectra of PEG-coated gold nanoparticles localized in extracellular matrix (HUVEC+GNRout) and internalized by HUVEC cells (HUVEC+GNRin) as detected by all-optical, narrow-beam PA spectrophotometer. Reproduced from open-source publication [22].

2.3.3 Identifying photoacoustic properties of target nanoagents in complex media

The future work on the detection and treatment of pancreatic cancer with PA will include investigation of theranostic nanoagents that have potential to provide specific molecular-targeted PA imaging of malignant tumor, PA and US activation of nanoagents, and following treatment of lesions.

Photoacoustic properties include (a) thermoelastic behavior of a system of an absorbing compound in complex surrounding environment and (b) absorption spectrum of nanoagents involved in biological processes. Petrova et al. [55] demonstrated that generation of PA response from blood in terms of its thermoelastic properties depends on compartmentalization of hemoglobin within erythrocyte. Recently, Pelivanov et al. [22] showed that localization of nanoagents in extracellular and/or intracellular matrix can affect the resultant absorption spectrum of nanoagents (**Figure 8**).

To identify thermoelastic and optical properties of PA contrast agents meticulously is crucial for successful implementation of theranostic nanoparticles for the therapy and early diagnostics of pancreatic cancer.

3. Conclusions

In summary, PA imaging is an emerging modality in gastroenterology and mostly used in combination with ultrasound or fluorescent imaging. Diagnosis through angiogenesis and blood oxygenation in the lining of esophagus and colon can be performed using PA imaging. High-resolution, multispectral PA imaging is offered via catheter-based (i) all-optical/noncontact solution and (ii) a miniaturized contact PA/US endoscope for preclinical studies. The capability to image both the mucosa and submucosa layers (up to 3–4 mm in depth of GI tract walls) is the vast advantage of these PA methods comparing to other routinely used optical imaging modalities. However, further miniaturization of catheter-based endoscopes and improvement on specificity of diagnostics through blood oxygenation parameters are required. Multispectral, multiscale PA/US system based on hand-held probe demonstrated rigorous data on assessment of a chronic inflammatory bowel disease in clinical studies. Using multispectral transabdominal examination, the PA system was able to evaluate hemoglobin level and blood oxygenation and accurately correlate it with abnormal activities in the large bowel and small intestine assessed through standard colonoscopic procedure. The only limitation of this method is depth beyond 5–6 cm in the body. Nonetheless, the proposed PA approach is noninvasive and use non-ionized radiation that is extremely fascinating for further clinical research. Many other PA imaging methods including intraoperative multimodality of PA and fluorescent imaging are currently under development and demonstrate high potential for use in gastroenterology.

Acknowledgements

This work was supported in part by the National Institutes of Health (National Cancer Institute) grant R01 CA181275.

Conflict of interest

The authors declare that there are no conflicts of interest on the presented manuscript.

IntechOpen

IntechOpen

Author details

Sheena Bhushan, Sharmila Anandasabapathy and Elena Petrova*
Baylor College of Medicine, Houston, Texas, USA

*Address all correspondence to: elena.petrova@bcm.edu

IntechOpen

© 2019 The Author(s). Licensee IntechOpen. This chapter is distributed under the terms of the Creative Commons Attribution License (<http://creativecommons.org/licenses/by/3.0>), which permits unrestricted use, distribution, and reproduction in any medium, provided the original work is properly cited. 

References

- [1] Loukas M, Tubbs RS, Benninger B. *Gastrointestinal Tract. Gray's Clinical Photographic Dissector of the Human Body*. 2nd ed. Elsevier Health Sciences; 2018. pp. 198-222. DOI: 10.1016/b978-1-4377-2417-2.00015-5
- [2] EBJ CV, Mouen K, Raman MV. In: Chandrasekhara V, editor. *Clinical Gastrointestinal Endoscopy*. 3rd ed. Philadelphia, Pennsylvania, USA: Elsevier; 2019
- [3] Knyrim K, Seidlitz H, Vakil N, Classen M. Perspectives in "electronic endoscopy". Past, present and future of fibers and CCDs in medical endoscopes. *Endoscopy*. 1990;22(Suppl 1):2. DOI: 10.1055/s-2007-1012877
- [4] Bruno MJ. Magnification endoscopy, high resolution endoscopy, and chromoscopy; towards a better optical diagnosis. *Gut*. 2003;52(Suppl 4):iv7-iv11. DOI: 10.1136/gut.52.suppl_4.iv7
- [5] Wong Kee Song LM, Adler DG, Chand B, Conway JD, Croffie JMB, DiSario JA, et al. Chromoendoscopy. *Gastrointestinal Endoscopy*. 2007;66(4):639-649. DOI: 10.1016/j.gie.2007.05.029
- [6] McGill SK, Evangelou E, Ioannidis JPA, Soetikno RM, Kaltenbach T. Narrow band imaging to differentiate neoplastic and non-neoplastic colorectal polyps in real time: A meta-analysis of diagnostic operating characteristics. *Gut*. 2013;62(12):1704-1713. DOI: 10.1136/gutjnl-2012-303965
- [7] Tan NC-W, Herd MK, Brennan PA, Puxeddu RBJO, Surgery M. The role of narrow band imaging in early detection of head and neck cancer. *British Journal of Oral and Maxillofacial Surgery*. 2012;50(2):132-136. DOI: 10.1016/j.bjoms.2010.12.001
- [8] Kiesslich R, Goetz M, Neurath MF. Virtual histology. *Best Practice & Research Clinical Gastroenterology*. 2008;22(5):883-897. DOI: 10.1016/j.bpg.2008.05.003
- [9] Goetz M, Watson A, Kiesslich R. Confocal laser endomicroscopy in gastrointestinal diseases. *Journal of Biophotonics*. 2011;4(7-8):498-508. DOI: 10.1002/jbio.201100022
- [10] Giovannini M, Caillol F, Monges G, Poizat F, Lemaistre A-I, Pujol B, et al. Endoscopic ultrasound-guided needle-based confocal laser endomicroscopy in solid pancreatic masses. *Endoscopy*. 2016;48(10):892-898. DOI: 10.1055/s-0042-112573
- [11] Wallace MB, Meining A, Canto MI, Fockens P, Miehlke S, Roesch T, et al. The safety of intravenous fluorescein for confocal laser endomicroscopy in the gastrointestinal tract. *Alimentary Pharmacology & Therapeutics*. 2010;31(5):548-552. DOI: 10.1111/j.1365-2036.2009.04207.x
- [12] Izatt JA, Kulkarni MD, Hsing-Wen W, Kobayashi K, Sivak MV. Optical coherence tomography and microscopy in gastrointestinal tissues. *IEEE Journal of Selected Topics in Quantum Electronics*. 1996;2(4):1017-1028. DOI: 10.1109/2944.577331
- [13] Yelbuz TM, Choma MA, Thrane L, Kirby ML, Izatt JA. Optical coherence tomography: A new high-resolution imaging technology to study cardiac development in chick embryos. *Circulation*. 2002;106(22):2771-2774. DOI: 10.1161/01.cir.0000042672.51054.7b
- [14] Hatta W, Uno K, Koike T, Yokosawa S, Iijima K, Imatani A, et al. Optical coherence tomography for the staging of tumor infiltration in superficial esophageal squamous cell

- carcinoma. *Gastrointestinal Endoscopy*. 2010;**71**(6):899-906. DOI: 10.1016/j.gie.2009.11.052
- [15] Rösch T. Endoscopic ultrasonography: Imaging and beyond. *Gut*. 2003;**52**(8):1220-1226. DOI: 10.1136/gut.52.8.1220
- [16] Cho CM. Training in endoscopy: Endoscopic ultrasound. *Clinical Endoscopy*. 2017;**50**(4):340-344. DOI: 10.5946/ce.2017.067
- [17] Gusev VE, Karabutov AA. *Laser Optoacoustics*. New York: American Institute of Physics; 1993. p. 136. DOI: 0.1021/acsnano.7b01032
- [18] Wang LV, SJs H. Photoacoustic tomography: In vivo imaging from organelles to organs. *Science*. 2012;**335**(6075):1458-1462. DOI: 10.1126/science.1216210
- [19] Petrova E, Liopo A, Oraevsky AA, Ermilov SA. Temperature-dependent optoacoustic response and transient through zero Grüneisen parameter in optically contrasted media. *Photoacoustics*. 2017;**7**:36-46. DOI: 10.1016/j.pacs.2017.06.002
- [20] Petrova EV, Brecht HP, Motamedi M, Oraevsky AA, Ermilov SA. In vivo optoacoustic temperature imaging for image-guided cryotherapy of prostate cancer. *Physics in Medicine & Biology*. 2018;**63**(6):064002. DOI: 10.1088/1361-6560/aab241
- [21] Oraevsky AA, Karabutov AA. *Optoacoustic Tomography*. Boca Raton, London, New York, Washington, DC: CRC Press; 2003. DOI: 10.1117/12.910975
- [22] Pelivanov I, Petrova E, Yoon SJ, Qian Z, Guye K, O'Donnell M. Molecular fingerprinting of nanoparticles in complex media with non-contact photoacoustics: Beyond the light scattering limit. *Scientific Reports*. 2018;**8**(1):14425. DOI: 10.1038/s41598-018-32580-2
- [23] Pelivanov I, Buma T, Xia J, Wei C-W, O'Donnell M. A new fiber-optic non-contact compact laser-ultrasound scanner for fast non-destructive testing and evaluation of aircraft composites. *Journal of Applied Physics*. 2014;**115**(11):113105. DOI: 10.1063/1.4868463
- [24] Wang L, Maslov K, Wang LV. Single-cell label-free photoacoustic flowoxigraphy in vivo. *Proceedings of the National Academy of Sciences of the United States of America*. 2013;**110**(15):5759-5764. DOI: 10.1073/pnas.1215578110
- [25] Runge TM, Abrams JA, Shaheen NJ. Epidemiology of Barrett's esophagus and esophageal adenocarcinoma. *Gastroenterology clinics of North America*. 2015;**44**(2):203-231. DOI: 10.1016/j.gtc.2015.02.001
- [26] Rastogi A, Puli S, El-Serag HB, Bansal A, Wani S, Sharma P. Incidence of esophageal adenocarcinoma in patients with Barrett's esophagus and high-grade dysplasia: A meta-analysis. *Gastrointestinal Endoscopy*. 2008;**67**(3):394-398. DOI: 10.1016/j.gie.2007.07.019
- [27] Mansour NM, Groth SS, Anandasabapathy S. Esophageal adenocarcinoma: Screening, surveillance, and management. *Annual Review of Medicine*. 2017;**68**(1):213-227. DOI: 10.1146/annurev-med-050715-104218
- [28] Muthusamy VR, Kim S, Wallace MB. Advanced imaging in Barrett's esophagus. *Gastroenterology Clinics of North America*. 2015;**44**(2):439-458. DOI: 10.1016/j.gtc.2015.02.012
- [29] Ansari R, Zhang EZ, Desjardins AE, Beard PC. All-optical forward-viewing photoacoustic probe for high-resolution

- 3D endoscopy. *Light: Science & Applications*. 2018;**7**(1):75. DOI: 10.1038/s41377-018-0070-5
- [30] Yang JM, Favazza C, Yao J, Chen R, Zhou Q, Shung KK, et al. Three-dimensional photoacoustic endoscopic imaging of the rabbit esophagus. *PLoS One*. 2015;**10**(4):e0120269. DOI: 10.1371/journal.pone.0120269
- [31] Lim L, Streutker CJ, Marcon N, Cirocco M, Lao A, Iakovlev VV, et al. A feasibility study of photoacoustic imaging of ex vivo endoscopic mucosal resection tissues from Barrett's esophagus patients. *Endoscopy International Open*. 2017;**5**(8):E775-E783. DOI: 10.1055/s-0043-111790
- [32] Ng SC, Shi HY, Hamidi N, Underwood FE, Tang W, Benchimol EI, et al. Worldwide incidence and prevalence of inflammatory bowel disease in the 21st century: A systematic review of population-based studies. *The Lancet*. 2017;**390**(10114):2769-2778. DOI: 10.1016/S0140-6736(17)32448-0
- [33] Bhutiani N, Grizzle WE, Galandiuk S, Otali D, Dryden GW, Egilmez NK, et al. Noninvasive imaging of colitis using multispectral optoacoustic tomography. *Journal of Nuclear Medicine: Official Publication, Society of Nuclear Medicine*. 2017;**58**(6):1009-1012. DOI: 10.2967/jnumed.116.184705
- [34] Knieling F, Neufert C, Hartmann A, Claussen J, Urich A, Egger C, et al. Multispectral optoacoustic tomography for assessment of Crohn's disease activity. *The New England Journal of Medicine*. 2017;**376**(13):1292-1294. DOI: 10.1056/NEJMc1612455
- [35] Waldner MJ, Knieling F, Egger C, Morscher S, Claussen J, Vetter M, et al. Multispectral optoacoustic tomography in Crohn's disease: Noninvasive imaging of disease activity. *Gastroenterology*. 2016;**151**(2):238-240. DOI: 10.1053/j.gastro.2016.05.047
- [36] Bray F, Ferlay J, Soerjomataram I, Siegel RL, Torre LA, Jemal A. Global cancer statistics 2018: GLOBOCAN estimates of incidence and mortality worldwide for 36 cancers in 185 countries. *CA: A Cancer Journal for Clinicians*. 2018;**68**(6):394-424. DOI: 10.3322/caac.21492
- [37] Hidalgo M, Cascinu S, Kleeff J, Labianca R, Löhner JM, Neoptolemos J, et al. Addressing the challenges of pancreatic cancer: Future directions for improving outcomes. *Pancreatology*. 2015;**15**(1):8-18. DOI: 10.1016/j.pan.2014.10.001
- [38] Stathis A, Moore MJ. Advanced pancreatic carcinoma: Current treatment and future challenges. *Nature Reviews Clinical Oncology*. 2010;**7**:163. DOI: 10.1038/nrclinonc.2009.236
- [39] Bassi C, Salvia R, Butturini G, Marcucci S, Barugola G, Falconi M. Value of regional lymphadenectomy in pancreatic cancer. *HPB : The Official Journal of the International Hepato Pancreato Biliary Association*. 2005;**7**(2):87-92. DOI: 10.1080/13651820510028855
- [40] Wagner M, Redaelli C, Lietz M, Seiler CA, Friess H, Büchler MW. Curative resection is the single most important factor determining outcome in patients with pancreatic adenocarcinoma. *BJS*. 2004;**91**(5):586-594. DOI: 10.1002/bjs.4484
- [41] Verbeke CS, Gladhaug IP. Resection margin involvement and tumour origin in pancreatic head cancer. *The British Journal of Surgery*. 2012;**99**(8):1036-1049. DOI: 10.1002/bjs.8734
- [42] Bronstein YL, Loyer EM, Kaur H, Choi H, David C, DuBrow RA, et al. Detection of small pancreatic tumors with

- multiphasic helical CT. *American Journal of Roentgenology*. 2004;**182**(3):619-623. DOI: 10.2214/ajr.182.3.1820619
- [43] Vahrmeijer AL, Hutteman M, Van Der Vorst JR, Van De Velde CJ, Frangioni JV. Image-guided cancer surgery using near-infrared fluorescence. *Nature Reviews Clinical Oncology*. 2013;**10**(9):507. DOI: 10.1038/nrclinonc.2013.123
- [44] Kruskal J, Kane R. Intraoperative ultrasonography of the pancreas: Techniques and clinical applications. *Surgical Technology International*. Bellingham, Washington, USA. 1997;**6**:49-57. DOI: 10.1148/rg.307105051
- [45] Sun MR, Brennan DD, Kruskal JB, Kane RA. Intraoperative ultrasonography of the pancreas. *Radiographics*. 2010;**30**(7):1935-1953. DOI: 10.15557/JoU.2015.0005
- [46] Hata S, Imamura H, Aoki T, Hashimoto T, Akahane M, Hasegawa K, et al. Value of visual inspection, bimanual palpation, and intraoperative ultrasonography during hepatic resection for liver metastases of colorectal carcinoma. *World Journal of Surgery*. 2011;**35**(12):2779-2787. DOI: 10.1097/01.sla.0000171307.37401.db
- [47] Handgraaf HJ, Boonstra MC, Van Erkel AR, Bonsing BA, Putter H, Van De Velde CJ, et al. Current and future intraoperative imaging strategies to increase radical resection rates in pancreatic cancer surgery. *Biomed Research International*. 2014;**2014**:8. Article ID: 890230. DOI: 10.1155/2014/890230
- [48] Nelson DW, Blanchard TH, Causey MW, Homann JF, Brown TA. Examining the accuracy and clinical usefulness of intraoperative frozen section analysis in the management of pancreatic lesions. *American Journal of Surgery*. 2013;**205**(5):613-617. DOI: 10.1016/j.amjsurg.2013.01.015
- [49] Harris PL, Rumley TO, Lineaweaver WC. Pancreatic cancer: Unreliability of frozen section in diagnosis. *Southern Medical Journal*. 1985;**78**(9):1053-1056. DOI: 10.1097/00007611-198509000-00007
- [50] Witz M, Shkolnik Z, Dinbar A. Intraoperative pancreatic biopsy—A diagnostic dilemma. *Journal of surgical oncology*. 1989;**42**(2):117-119. DOI: 10.1002/jso.2930420210
- [51] Homan K, Shah J, Gomez S, Gensler H, Karpiouk A, Brannon-Peppas L, et al. Combined Ultrasound and Photoacoustic Imaging of Pancreatic Cancer Using Nanocage Contrast Agents. *Proceeding SPIE, Photons Plus Ultrasound: Imaging and Sensing*. 2009; 71771M, 6 p. DOI: 10.1117/12.807520
- [52] Homan KA, Souza M, Truby R, Luke GP, Green C, Vreeland E, et al. Silver nanoplate contrast agents for in vivo molecular photoacoustic imaging. *ACS Nano*. 2012;**6**(1):641-650. DOI: 10.1021/nn204100n
- [53] Dai X, Qian W, Yang H, Yang L, Jiang H. Targeted molecular imaging of pancreatic cancer with a miniature endoscope. *Applied Sciences*. 2017;**7**(12):1241. DOI: 10.3390/app7121241
- [54] Tummers WS, Miller SE, Teraphongphom NT, Gomez A, Steinberg I, Huland DM, et al. Intraoperative pancreatic cancer detection using tumor-specific multimodality molecular imaging. *Annals of Surgical Oncology*. 2018;**25**(7):1880-1888. DOI: 10.1245/s10434-018-6453-2
- [55] Petrova EV, Oraevsky AA, Ermilov SA. Red blood cell as a universal optoacoustic sensor for non-invasive temperature monitoring. *Applied Physics Letters*. 2014;**105**(9):094103. DOI: 10.1063/1.4894635